Inorg. Chem. **2002**, *41*, 1263–1271

Trinuclear Pyrazine-Bridged Ruthenium Complexes: Syntheses, Electrochemistry, NIR–Vis Spectra, and Their Interpretation in Terms of a 5-Orbital–3-Parameter Model

Milena Sommovigo,[†] Alessandro Ferretti,*[,‡] Margherita Venturi,[§] Paola Ceroni,[§] Cecilia Giardi,[†] and Gianfranco Denti*[,†]

Dipartimento di Chimica e Biotecnologie Agrarie, Università di Pisa, Via del Borghetto 80, I-56124 Pisa, Italy, and Istituto di Chimica Quantistica ed Energetica Molecolare del CNR, Area della Ricerca, Via G. Moruzzi 1, I-56010 Ghezzano (Pisa), Italy, and Dipartimento di Chimica "G. Ciamician", Università di Bologna, Via Selmi 2, I-40126 Bologna, Italy

Received August 13, 2001

A study of absorption spectra in the near-infrared (NIR) and visible (vis) regions of trinuclear Ru complexes containing pyrazine (pyz) as bridging ligand, *trans*-$[\{Ru(NH_3)_5pyz\}_2Ru(NH_3)_4]^{m+}$ ($m = 6$–9), is reported. The spectra were recorded on aqueous solutions containing the described species formed in situ by stoichiometric additions of a standard solution of $Ce(SO_4)_2$. They were interpreted in terms of a simple 5-orbital–3-parameter model which includes the effects of d–π^* interaction and electronic correlation. The model is shown to account for the observed NIR–vis spectra of the complex ions. The 6+ parent species was synthesized by an improved literature method and fully characterized. The novel 8+ complex was also prepared and characterized. The 9+ ion was established to be slowly reduced by water, with dioxygen formation. Electrochemical (CV and DPV) studies were performed on the trinuclear 6+ complex, as well as on its constituent fragments $[Ru(NH_3)_5(pyz)]^{2+}$ and *trans*-$[Ru(NH_3)_4(pyz)_2]^{2+}$.

Introduction

Medium sized molecular systems, displaying efficient intramolecular electron and/or energy transfer, have attracted a large interest owing to their potential applications in electronic devices at the molecular level. On one hand, electronic energy transfer[1] which is associated with reversible light-to-energy conversion, such as absorption and emission processes, can be exploited for the transmission and/or processing of light signals; on the other hand, molecules in which one or more unpaired electrons can be delocalized become easily polarizable and may exhibit interesting nonlinear optical[2,3] or magnetic[4] properties, behave as conductors or semiconductors,[5] and even show bistability with hysteresis.[6]

The study of electron transfer, which has been given a substantial boost by the work by Marcus and Hush,[7] is per

* Authors to whom correspondence should be addressed. E-mail: gdenti@agr.unipi.it (G.D.); ferretti@icqem.pi.cnr.it (A.F.).
† Università di Pisa.
‡ CQEM-CNR.
§ Università di Bologna.

(1) (a) Balzani, V.; Scandola, F. *Supramolecular Photochemistry*; Horwood: Chichester, U.K., 1991. (b) Schlike, B.; Belser, P.; De Cola, L.; Sabbioni, E.; Balzani, V. *J. Am. Chem. Soc.* **1999**, *121*, 4207. (c) Flamigni, L.; Barigelletti, F.; Armaroli, N.; Collin, J.-P.; Dixon, I. M.; Sauvage, J.-P.; Gareth Williams, J. A. *Coord. Chem. Rev.* **1999**, *190*, 0−192, 671.

(2) (a) Prasad, P. N.; Williams, D. J. *Introduction to Nonlinear Optical Effects in Molecules & Polymers*; John Wiley & Sons: New York, 1991. (b) *Nonlinear Optical Materials*: *Theory and Modelling*; Karna, S. P., Yeates, A. T., Eds.; ACS Symposium Series 628; American Chemical Society: Washington, DC, 1996.

(3) (a) Ferretti, A.; Lami, A.; Villani, G. *J. Phys. Chem. A* **1997**, *101*, 9439. (b) Sheadi, I. A.; Murga, L. F.; Ondrechen, M. J.; Lindergerg, J. *Chem. Phys. Lett.* **1998**, *291*, 325.

(4) Bencini, A.; Palii, A. V.; Ostrovsky, S. M.; Tsukerblat, B. S.; Uytterhoeven, M. G. *Mol. Phys.* **1995**, *86*, 1085. (b) Bominaar, E. L.; Achim, C.; Borshch, S. A.; Gired, J.-J.; Münck, E. *Inorg. Chem.* **1997**, *36*, 3689. (c) Barone, V.; Bencini, A.; Ciofini, I.; Daul, C. A.; Totti, F. *J. Am. Chem. Soc.* **1998**, *120*, 8357. (d) Borrás-Almenar, J. J.; Coronado, E. Ostrovsky, S. M.; Palii, A. V.; Tsukerblat, B. S. *Chem. Phys. Lett.* **1999**, *240*, 149. (e) Belinsky, M. I. *Chem. Phys. Lett.* **1999**, *240*, 303.

(5) (a) Hanack, M.; Deger, S.; Lange, A. *Coord. Chem. Rev.* **1988**, *83*, 11. (b) Hanack, M. *Mol. Cryst. Liq. Cryst.* **1988**, *160*, 133. (c) Hanack, M.; Lang, M. *Adv. Mater.* **1994**, *6*, 819.

(6) Tomita, A.; Sano, M. *Inorg. Chem.* **2000**, *39*, 200.

10.1021/ic010869y CCC: $22.00
Published on Web 02/14/2002

se of fundamental importance in all scientific disciplines, from biology to physics. This explains the intense activity that still characterizes the field, well documented in several review or feature articles.[8] However, from the point of view of potential technological applications, the intramolecular process that takes place when electron donor (D) and electron acceptor (A) units are bound within the same molecular species, directly or through a bridge (B), should be regarded with special attention in order to reveal the possible appearance of the previously mentioned properties.

In this perspective, when D and A are transition metal complexes that can be oxidized or reduced and B is a bridging heteroaromatic ligand, a whole class of compounds is available in which electron transfer may be chemically or electrochemically tuned. Thus, one can also construct symmetric systems where D and A have the same chemical nature but the metals are in different oxidation states; these are the so-called mixed-valence (MV) compounds, in which the electronic charge can be delocalized on the whole molecule through suitable bridging ligands.

These compounds are very well-known and widely studied since the first theoretical approach by Hush[9] and the pioneering experimental work by Creutz and Taube[10] on the pyrazine-bridged Ru pentaammine dinuclear species. To date, a large variety of dinuclear MV compounds have been prepared and studied. Besides the extensive collections and discussions which can be found in review articles,[11] in the past few years several papers on the subject have been published by various groups, dealing with different metals and/or bridging ligands.[12−18]

With the aim of investigating the extent of metal−metal interaction, several theoretical attempts have been made to reproduce and explain the observed NIR−vis optical properties, these indeed being related to the electron delocalization that metal−metal coupling can induce. The early two-state Hush model[9b] and its full vibronic counterpart, the Piepho−Krausz−Schatz (PKS) model,[19] have first established the connection between relevant molecular parameters and the observed position, intensity, and line shape profile of the NIR metal−metal charge transfer (or intervalence) band. These models have been later generalized in order to take into account the effects of ligand orbitals,[20,21] also in view of studying complexes containing bridges of different lengths.[22] Indeed, for the Creutz−Taube ion (the 5+ pyrazine-bridged Ru pentaammine dinuclear species), the X_α study by Ondrechen and co-workers[23] has demonstrated the importance of, besides the metal d orbitals, the empty π^* ligand orbital. Superexchange models[8a,11b,13] have been applied to the study of several mixed-valence complexes, also including the dependence of matrix elements from nuclear coordinates.[17]

The effects of coupling between electronic and nuclear degrees of freedom constitute a very interesting research subject and have been discussed in several articles by different authors.[9b,17−20,23b−26] For a delocalized system, such as the Creutz−Taube ion, the ground state in the (Ru_1−pyz, Ru_2−pyz) plane is found to be a paraboloid,[27] so that the vibronic coupling mainly affects the line shape profile of the bands, which is relevant for the computation of electroabsorption spectra.[28] On the other hand, in localizable systems, the coupling with nuclear degrees of freedom may localize the unpaired electron[9b,19,29] on a specific fragment.

Most of the work is related to bimetallic species, which can be currently examined also by ab initio theoretical methods.[27,30] Despite the relevance for possible applications in molecular devices, investigations of the dependence of

(7) (a) Marcus, R. A. *J. Chem. Phys.* **1956**, *24*, 966. (b) Hush, N. S. *Trans. Faraday Soc.* **1961**, *57*, 155.
(8) (a) Newton, M. D. *Chem. Rev.* **1991**, *91*, 767. (b) Barbara, P. F.; Meyer, T. J.; Ratner, M. A. *J. Phys. Chem.* **1996**, *100*, 13148. (c) Davis, W. B.; Svec, W. A.; Ratner, M. A.; Wasielewski, M. R. *Nature* **1998**, *396*, 60.
(9) (a) Allen, G. C.; Hush, N. S. *Prog. Inorg. Chem.* **1967**, *8*, 357. (b) Hush, N. S. *Prog. Inorg. Chem.* **1967**, *8*, 391.
(10) Creutz, C.; Taube, H. *J. Am. Chem. Soc.* **1969**, *91*, 3988.
(11) (a) Creutz, C. *Prog. Inorg. Chem.* **1983**, *30*, 1. (b) Crutchley, R. J. *Adv. Inorg. Chem.* **1994**, *41*, 273. (c) Endicott, J. F.; Watzky, M. A.; Song, X.; Buranda, T. *Coord. Chem. Rev.* **1997**, *159*, 295. (d) Demadis, K. D.; Hartshorn, C. M.; Meyer, T. J. *Chem. Rev.* **2001**, *101*, 2655.
(12) (a) Almaraz, A. E.; Gentil, L. A.; Baraldo, L. M.; Olabe, J. A. *Inorg. Chem.* **1996**, *35*, 7718. (b) Almaraz, A. E.; Gentil, L. A.; Baraldo, L. M.; Olabe, J. A. *Inorg. Chem.* **1997**, *36*, 1517. (c) Hornung, M. F.; Bauman, F.; Kaim, W.; Olabe, J. A.; Slep, L. D.; Fiedler, J. *Inorg. Chem.* **1998**, *37*, 311.
(13) (a) Rezvani, A. R.; Bensimon, C.; Cromp, B.; Reber, C.; Greedan, J. E.; Kondratiev, V. V.; Crutchley, R. J. *Inorg. Chem.* **1997**, *36*, 3322. (b) Nacklicki, M. L.; White, C. A.; Plante, L. L.; Evans, C. E. B.; Crutchley, R. J. *Inorg. Chem.* **1998**, *37*, 1880.
(14) Richardson, G. N.; Brand, U.; Vahrenkamp, H. *Inorg. Chem.* **1999**, *38*, 3070.
(15) Glöckle, M.; Kaim, W.; Katz, N. E.; Posse, M. G.; Cutin, E. H.; Fiedler, J. *Inorg. Chem.* **1999**, *38*, 3270.
(16) Demadis, K. D.; Neyhart, G. A.; Kober, E. M.; White, P. S.; Meyer, T. J. *Inorg. Chem.* **1999**, *38*, 5948.
(17) (a) Watzky, M. A.; Macatangay, A. V.; Van Camp, R. A.; Mazzetto, S. E.; Song, X.; Endicott, J. F. *J. Phys. Chem. A* **1997**, *101*, 8441. (b) Macatangay, A. V.; Endicott, J. F.; Song, X. *J. Phys. Chem. A* **1998**, *102*, 7537. (c) Macatangay, A. V.; Mazzetto, S. E.; Endicott, J. F. *Inorg. Chem.* **1999**, *38*, 5091. (d) Endicott, J. F.; Macatangay, A. V. *Inorg. Chem.* **2000**, *39*, 437.
(18) Geiss, A.; Kolm, M. J.; Janiak, C.; Vahrenkam, H. *Inorg. Chem.* **2000**, *39*, 4037 and reference therein.
(19) (a) Piepho, S. B.; Krausz, E. R.; Schatz, P. N. *J. Am. Chem. Soc.* **1978**, *100*, 2996. (b) Wong, K. Y.; Schatz, P. N. *Prog. Inorg. Chem.* **1981**, *28*, 369.
(20) (a) Piepho, S. B. *J. Am. Chem. Soc.* **1988**, *110*, 6319. (b) Piepho, S. B. *J. Am. Chem. Soc.* **1990**, *112*, 4197.
(21) Cave, R. J.; Newton, M. D. *Chem. Phys. Lett.* **1996**, *249*, 15.
(22) (a) Reimers, J. R.; Hush, N. S. *Inorg. Chem.* **1990**, *29*, 3686. (b) Reimers, J. R.; Hush, N. S. *Inorg. Chem.* **1990**, *29*, 4510.
(23) (a) Zhang, L.-T.; Ko, J.; Ondrechen, M. J. *J. Am. Chem. Soc.* **1987**, *109*, 1666. (b) Ondrechen, M. J.; Ko, J.; Zhang, L.-T. *J. Am. Chem. Soc.* **1987**, *109*, 1672.
(24) Prassides, K.; Schatz, P. N.; Wong, K. Y.; Day, P. *J. Phys. Chem.* **1986**, *90*, 5588.
(25) Reimers, J. R.; Hush, N. S. *Chem. Phys.* **1996**, *208*, 177.
(26) (a) Ferretti, A.; Lami, A.; Ondrechen, M. J.; Villani, G. *J. Phys. Chem.* **1995**, *99*, 10484. (b) Erratum: Ferretti, A.; Lami, A.; Ondrechen, M. J.; Villani, G. *J. Phys. Chem.* **1996**, *100*, 20174.
(27) Bencini, A.; Ciofini, I.; Daul, C. A.; Ferretti, A. *J. Am. Chem. Soc.* **1999**, *121*, 11418.
(28) (a) Reimers, J. R.; Hush, N. S. *J. Phys. Chem.* **1991**, *95*, 9773. (b) Murga, L. F.; Ferretti, A.; Lami, A.; Ondrechen, M. J.; Villani, G. *Inorg. Chem. Commun.* **1998**, *1*, 137. (c) Ferretti, A.; Lami, A.; Murga, L. F.; Shehadi, I. A.; Ondrechen, M. J.; Villani, G. *J. Am. Chem. Soc.* **1999**, *121*, 2594.
(29) Ferretti, A.; Improta R.; Lami, A.; Villani, G. *J. Phys. Chem. A* **2000**, *104*, 9591.
(30) (a) Sizova, O. V.; Baranovski, V. I.; Ivanova, N. V.; Panin, A. I. *Int. J. Quantum Chem.* **1997**, *63*, 853. (b) Metcalife, R. A.; Vasconcellos, L. C. G.; Mirza, H.; Franco, D. W.; Lever, A. B. P. *J. Chem. Soc., Dalton Trans.* **1999**, *118*, 2653. (c) Hush, N. S.; Reimers, J. R. *J. Phys. Chem. A* **1999**, *103*, 3066. (d) Masui, H.; Freda, A. L.; Zerner, M. C.; Lever, A. B. P. *Inorg. Chem.* **2000**, *39*, 141. (e) Cacelli, I.; Ferretti, A.; Toniolo, A. *J. Phys. Chem. A* **2001**, *105*, 4480.

the NIR−vis optical properties on the nuclearity of the complexes are rather scarce, and extensive experimental studies have been carried out for cyanide bridged trimetallic species only.[17,31] As far as polynuclear pyrazine-bridged Ru complexes are concerned, after the 1978 work by Von Kameke, Tom, and Taube,[32] no further investigations have been carried out. The strong metal−metal interaction, observed in the corresponding mixed-valence bimetallic complex,[10] confers particular interest to new studies.

In this perspective, we thought that it was worthwhile to examine the trinuclear ruthenium ions [*trans*-{$Ru(NH_3)_5$-pyz}$_2$$Ru(NH_3)_4$]$^{m+}$ (Ru_3^{m+}; $m = 6-9$). These species have been synthesized by a modification of the Von Kameke−Tom−Taube procedures:[32] better yields in Ru_3^{6+} were obtained, and a salt of the oxidized form Ru_3^{8+} was also synthesized. Both complexes were fully characterized by elemental and spectrometric analysis, the former as hexafluorophosphate (Ru_3^{6+}−P) and tetraphenylborate (Ru_3^{6+}−B) salts, the latter as sulfate/bisulfate mixed salt.

The electrochemistry (CV and DPV) of Ru_3^{6+} and of its constituent fragments, $[Ru(NH_3)_5(pyz)]^{2+}$ and *trans*-[Ru-$(NH_3)_4(pyz)_2]^{2+}$, was studied in order to collect useful data for their characterization and, more importantly, to test the stability of the trinuclear species in different oxidation states.

NIR−vis spectra were recorded as a function of the total charge, which was increased by sequential stoichiometric oxidations of the Ru_3^{6+} compound. The measured spectra were then compared with those calculated by a simple electronic model, first applied to the computation of optical conductivity spectra.[33]

Experimental Section

Reagents. *trans*-$[Ru(NH_3)_4(SO_2)Cl]Cl$ and $[(NH_3)_5RuCl]Cl_2$ were prepared following the methods already known;[34] $[Ru(NH_3)_5$-$(pyz)]^{2+}$, synthesized as reported in the literature,[35] was isolated as its hexafluorophosphate salt. Solvents (HPLC grade) were used without further purification. Deionized water was distilled twice and degassed with argon before use. The following reagents were used as received: pyrazine, silver trifluoroacetate, ammonium hexafluorophosphate, sulfuric acid, sodium tetraphenylborate (Aldrich), hydrogen peroxide 35% (Baker), 0.1 M Ce(IV) sulfate standard solution (Riedel de Haën), hydrochloric acid, lithium chloride, sodium bicarbonate (Carlo Erba). Zinc amalgam was prepared by the standard method using granular zinc and $HgCl_2$ (Aldrich). Preparation of complexes was made under argon atmosphere using a standard Schlenk technique; filtrations and purifications were usually performed in air.

Electrochemical Measurements. Cyclic voltammetric (CV) and differential pulse voltammetric (DPV) experiments were carried out in argon-purged water (milliQ, 18.2 MΩ) at 22 °C with an Autolab 30 multipurpose instrument interfaced to a personal computer. The working electrode was a glassy carbon electrode (0.08 cm^2, Amel); its surface was routinely polished with a 0.05 μm alumina−water slurry on a felt surface, immediately prior to use. In all cases, the counter electrode was a Pt spiral, separated from the bulk solution with a fine glass frit, and the reference electrode was a saturated calomel electrode (SCE). The concentration of the compounds was on the order of 5×10^{-4} M; the experiments were carried out in the presence of H_2SO_4 (1.0 M) or sodium perchlorate (0.05 M). In the latter case, when necessary, the pH was adjusted with sulfuric acid. Cyclic voltammograms were obtained with sweep rates in the range 0.01−1 V s^{-1}; DPV experiments were performed with a scan rate of 20 or 4 mV s^{-1}, a pulse height of 75 or 10 mV, and a duration of 40 ms. The reversibility of the observed processes was established by using the criteria of (i) separation of 60 mV between cathodic and anodic peaks, (ii) close-to-unity ratio of the intensities of the cathodic and anodic currents, and (iii) constancy of the peak potential on changing sweep rate in the cyclic voltammograms. The same halfwave potential values were obtained from the DPV peaks and from an average of the cathodic and anodic CV peaks, as expected for reversible processes. The number of electrons exchanged in each process observed for the trinuclear compound was estimated by comparing the current intensity of the CV waves and the area of the DPV peaks with those obtained under the same conditions for the mononuclear complexes, after correction for differences in the diffusion coefficients.

Spectra. IR spectra (KBr pellets) were recorded with a Perkin-Elmer 1330 IR spectrophotometer. ^{1}H NMR spectra were recorded with a Bruker AC-200, using a D_2O solution of sodium 2,2-dimethyl-2-silapentane-5-sulfonate (DSS) as external reference for samples dissolved in D_2O and TMS as internal reference for those dissolved in trideuterioacetonitrile. The fine splitting of AA′BB′ pattern due to pyrazine hydrogens is not reported, so that *J* values only refer to the two most intense peaks. NIR−vis spectra were recorded in a 1 cm quartz cell with a Perkin-Elmer Lambda 19 spectrophotometer. Solutions (5 mL, 5×10^{-5} M) were prepared by dissolving the appropriate amount of Ru_3^{6+}−P in 1.0 M H_2SO_4 heavy water solution and then adding successive stoichiometric portions (2.5 μL) of a standard 0.1 M solution of $Ce(SO_4)_2$ (after each measurement the content of the cell was reunified to the mother solution in the graduated flask before adding the oxidant, so making the volume increment negligible).

Oxygen detection was made with a Hanna HI 9142 dissolved oxygen meter.

***trans*-$[Ru(NH_3)_4(pyz)_2]Cl_2$ (Ru_1).** The complex was prepared with few modifications of the procedure reported for the protonated analogue *trans*-$[Ru(NH_3)_4(Hpyz)_2]Cl_4$.[32] *trans*-$[Ru(NH_3)_4(SO_2)Cl]$-Cl (0.150 g, 0.44 mmol) and an excess of pyrazine (0.150 g, 1.88 mmol) were dissolved in water (3 mL), and the pH was adjusted to 7−8 using $NaHCO_3$ (∼0.130 g). The solution turned from orange to deep red. After 15 min under stirring in the dark, the solution was acidified with 1.0 M HCl until the CO_2 evolution ceased. H_2O_2 (35%) was then added under stirring until the solution turned from red to greenish brown (∼3 mL). After 10 min, acetone (100 mL) was added, and a yellow solid started to precipitate; the suspension was cooled in the refrigerator for 1 h. The precipitate so obtained was filtered out, washed with acetone, and vacuum-dried. It was dissolved in 0.01 M HCl (3 mL) and reacted with Zn amalgam (1.2 g) for 30 min. Pyrazine (0.700 g, 8.75 mmol) was then added, and the mixture stirred for 5 h in the dark. The solution turned reddish violet. Zn/Hg was removed by filtration, and LiCl (0.098 g, 2 mmol) and then acetone (75 mL) were added. The solution was refrigerated for 2 h, and the crude product so obtained was filtered out and vacuum-dried. It was then purified by chromatog-

(31) Scandola, F.; Indelli, M. T.; Chiorboli, C.; Bignozzi, C. A. In *Photoinduced Electron-Transfer II*; Mattay, J., Ed.; Springer: Berlin, 1990.
(32) Von Kameke, A.; Tom, G. M.; Taube, H. *Inorg. Chem.* **1978**, *17*, 1790.
(33) (a) Ferretti, A.; Lami, A. *Chem. Phys.* **1994**, *181*, 107. (b) Ferretti, A.; Lami, A. *Chem. Phys. Lett.* **1994**, *220*, 327. (c) Ferretti, A.; Lami, A.; Villani, G. *Inorg. Chem.* **1998**, *37*, 2799.
(34) Chang, J. P.; Fung, E. Y.; Curtis, J. C. *Inorg. Chem.* **1986**, *25*, 4233 and references therein.
(35) Creutz, C.; Taube, H. *J. Am. Chem. Soc.* **1973**, *95*, 1086.

raphy on a neutral alumina column (20 cm × 1.5 cm) with CH_3CN/MeOH 1:1 (v/v) as eluant, operating in subdued light. The first bright orange fraction was collected and rotary evaporated to a small volume. Upon addition of ethanol, Ru_1 was obtained as a red solid, which was filtered out, washed with ethanol, and vacuum-dried (0.131 g, 74% based on *trans*-$[Ru(NH_3)_4(SO_2)Cl]Cl$). Anal. Calcd for $C_8N_8H_{20}RuCl_2 \cdot 2H_2O$: N, 25.68; C, 22.00; H, 5.50. Found: N, 26.00; C, 21.78; H, 5.36. Vis: (H_2O, $\sim 1 \times 10^{-5}$ M) 485 nm; (0.2 M HCl, $\sim 1 \times 10^{-5}$ M) 550 nm.[32] ^{1}H NMR (D_2O, DSS external reference, ppm): 8.79 (4H, dd, $J = 4.2$ Hz, pyz), 8.52 (4H, dd, $J = 4.2$ Hz, pyz); 2.52 (s, NH_3). IR (KBr pellet, cm^{-1}): 3400 br, s [ν_{OH}]; 3300, 3220 br, s [ν_{NH}]; 1630 s, 1300 br, s [δ_{NH}]. IR (perdeuterated complex, KBr pellet, cm^{-1}): 2440 br, s [ν_{OD}]; 2380, 2300 br, s [ν_{ND}]; 1200 m, 1000 m [δ_{ND}].

***trans*-[{Ru(NH$_3$)$_5$pyz}$_2$Ru(NH$_3$)$_4$](PF$_6$)$_6$ (Ru$_3^{6+}$−P).** A mixture of $[(NH_3)_5RuCl]Cl_2$ (0.062 g, 0.21 mmol) and silver(I) trifluoroacetate (0.0936 g, 0.420 mmol) in water (3 mL) was digested at 80 °C until silver chloride coagulated. It was then cooled and filtered. The AgCl was washed with small portions of water, and the filtrate portions were combined and deoxygenated with argon in a Schlenk vessel. Freshly prepared zinc amalgam (~0.300 g) and Ru_1 (0.042 g, 0.105 mmol) were added. The mixture was stirred in the dark until the visible spectrum showed only the peak (630 nm) of the trinuclear compound. The dark blue solution was filtered and rotary evaporated to small volume. An excess of NH_4PF_6 (0.300 g, 1.840 mmol) and ethanol (30 mL) were added, and the mixture cooled overnight. The blue solid so obtained was filtered out and recrystallized from water/ethanol (blue powder, 0.150 g, 87%). When microcrystalline, the compound is green. Anal. Calcd for $C_8N_{18}H_{50}Ru_3P_6F_{36} \cdot EtOH$: N, 15.58; C, 7.42; H, 3.46. Found: N, 15.83; C, 7.67; H, 3.51. Vis (H_2O, $\sim 1 \times 10^{-3}$ M): 630 nm.[32] ^{1}H NMR (D_2O, DSS external reference, ppm): 8.55 (4H, dd, $J = 5$ Hz, pyz), 8.16 (4H, dd, $J = 5$ Hz, pyz); 3.64 (2 H, q, $J = 7.1$ Hz, CH_3CH_2OH); 2.52 (br, s, NH_3); 1.17 (3H, t, $J = 7.1$ Hz, CH_3CH_2OH). IR (KBr pellet, cm^{-1}): 3420 br, s [ν_{OH}]; 3300, 3240, 3180 br, s [ν_{NH}]; 1620 m, 1290 m [δ_{NH}]; 840 br, vs [ν_{PF}]. IR (deuterium exchanged complex, KBr pellet, cm^{-1}): 2520 br, s [ν_{OD}]; 2440, 2400, 2360 br, m [ν_{ND}]; 1200 m, 1000 m [δ_{ND}]; 840 br, vs [ν_{PF}].

***trans*-[{Ru(NH$_3$)$_5$pyz}$_2$Ru(NH$_3$)$_4$](BPh$_4$)$_6$ (Ru$_3^{6+}$−B).** Ru_3^{6+}−P (0.030 g 0.018 mmol) was dissolved in water (5 mL), and solid $NaBPh_4$ (0.060 g, 0.170 mmol) was added under stirring. The blue solid that precipitated was filtered out, washed with small portions of water, and vacuum-dried. Recrystallization from acetonitrile and ether gave the product (0.030 g, 63%). Anal. Calcd for $C_{152}N_{18}H_{170}Ru_3B_6$: N, 9.63; C, 69.73; H, 6.54. Found: N, 9.55; C, 70.02; H, 6.68. Vis (H_2O, $\sim 1 \times 10^{-3}$ M): 630 nm. ^{1}H NMR (CD_3CN, TMS internal reference, ppm): 8.26 (4H, dd, $J = 5$ Hz, pyz); 7.82 (4H, dd, $J = 5$ Hz, pyz); 7.43 (48 H, m, BPh_4, *meta H*); 7.14 (48 H, t, $J = 7$ Hz, BPh_4, *ortho H*); 6.98 (24 H, t, $J = 6.9$ Hz, BPh_4, *para H*); 2.90 (6 H, br s, *trans*-NH_3); 1.82 (24 H, br s, *cis*-NH_3, terminal ruthenium); 1.70 (12 H, br s, *cis*-NH_3, central ruthenium). IR (KBr pellet, cm^{-1}): 3300, 3240, 3180 br, s [ν_{NH}]; 3050 br, s [ν_{CH}]; 1620 s, 1300 s [δ_{NH}]; 1580, br, m [$\nu_{C=C}$].

***trans*-[{Ru(NH$_3$)$_5$pyz}$_2$Ru(NH$_3$)$_4$](SO$_4$)$_3$(HSO$_4$)$_2$ (Ru$_3^{8+}$).** A solution of cerium sulfate (0.1 N, 0.48 mL, 0.048 mmol) in 1.0 M H_2SO_4 (1 mL) was dropped into a stirred solution of Ru_3^{6+}−P (0.038 g, 0.024 mmol) in 1.0 M H_2SO_4 (3 mL). The color turned from blue to violet, and a violet solid started to precipitate. After stirring at room temperature for 2 h, the mixture was filtered; the solid was washed with small portions of water, and then with acetone, and vacuum-dried (0.0175 g, 56%). Anal. Calcd for $C_8N_{18}H_{52}Ru_3S_5O_{20} \cdot 6H_2O$: N, 19.51; C, 7.43; H, 4.95; S, 12.40. Found: N, 19.24; C, 7.50; H, 4.67; S, 12.40. Vis (1 M H_2SO_4, $\sim 1 \times 10^{-5}$ M): 569 nm. IR (KBr pellet cm^{-1}): 3420 br, s [ν_{OH}]; 3250, 3080 br, s [ν_{NH}]; 1620 m, 1310 m [δ_{NH}]; 1120 br, vs, 620 m [SO_4^{--}].

Oxidation of Water by Ru$_3^{9+}$. To produce the 9+ species in solution, Ru_3^{6+}−P (0.175 g, 0.110 mmol) and 1.0 M H_2SO_4 (3.0 mL), carefully deoxygenated with argon, were mixed in a three-necked flask fitted with an oxygen probe passing through a holed Suba seal, a rubber septum, and a stopcock joint connected to the argon line under pressure. Once the probe reached the equilibrium (0 ppm on the meter), to the blue solution, kept under stirring, was quickly added an excess of $Ce(SO_4)_2$ (0.1 M standard deoxygenated solution, 5 mL) through the septum with a syringe. The mixture became immediately yellow, and a yellow solid formed. After a few seconds (~30), the solution turned violet, and a loud gas evolution was observed while the level of dioxygen quickly rose, putting the meter out of scale (>20 ppm). After 3 days of stirring, the mixture contained a violet microcrystalline solid which was filtered out, washed with water, and then with acetone, vacuum-dried (0.140 g), and characterized as Ru_3^{8+}.

Results

Synthesis and Characterization. The synthetic procedures for obtaining, in high yields and purities, *trans*-$[Ru(NH_3)_4(pyz)_2]Cl_2$ (Ru_1) and *trans*-$[\{Ru(NH_3)_5pyz\}_2Ru(NH_3)_4]^{6+}$, both as hexafluorophosphate (Ru_3^{6+}−P) and tetraphenylborate (Ru_3^{6+}−B) salts, have been set up modifying the previously reported methods. Furthermore, *trans*-$[\{Ru(NH_3)_5pyz\}_2Ru(NH_3)_4]$ $(SO_4)_3(HSO_4)_2$ (Ru_3^{8+}) has been first synthesized and isolated.

Both complexes Ru_1 and Ru_3^{6+} are light sensitive in solution. Very diluted aqueous solutions (1×10^{-5} M) of Ru_1 exposed to sunlight turn from orange to pink and finally to pale yellow within 10 h. In similar conditions, Ru_3^{6+}−P completely decomposes in 3 days, while in the dark at 5 °C it is stable over months. The decomposition products have not been investigated.

NMR spectra of both complexes in D_2O (in usual organic solvents they are not soluble enough) exhibit an AA′BB′ pattern in the aromatic region consisting of two double doublets in the ratio 1:1, clearly accounting for a trans arrangement of pyrazine ligands. For both species, the absorption intensities of ammonia hydrogens are lower than expected. This is due to H/D exchange:[36] at room temperature, it goes to completeness in about 30 h for Ru_1 and in 30 min for Ru_3^{6+}. Furthermore, in the NMR spectrum of the latter complex in D_2O (where it is sparingly soluble), only one broad signal at 2.5 ppm is observed for all ammonia hydrogens.

To get a better NMR characterization of Ru_3^{6+} cation, its tetraphenylborate salt (Ru_3^{6+}−B) was prepared, which is soluble in d_3-acetonitrile. In this solvent, all signals of the different ammonia hydrogens are observed with the expected intensity; chemical shifts are in agreement with those reported[37] for similar compounds. The addition of a few microliters of D_2O results in their disappearance.

(36) Meyer, T. J.; Taube, H. *Inorg. Chem.* **1968**, *7*, 2369

(37) (a) Coe, B. J.; Harris, J. A.; Asselberghs, I.; Persoons, A.; Jeffery, J. C.; Rees, L. H.; Gelbrich, T.; Hursthouse, M. B. *J. Chem. Soc., Dalton Trans.* **1999**, *118*, 3617. (b) Tomita, A.; Sano, M. *Inorg. Chem.* **2000**, *39*, 200.

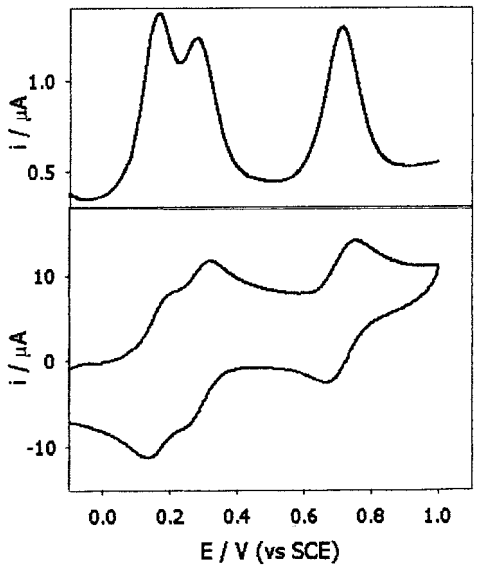

Figure 1. Electrochemical behavior on oxidation of the trinuclear compound (aqueous solution, 1.0 M H_2SO_4 , glassy carbon as working electrode and SCE as reference): differential pulse voltammogram at scan rate of 4 mV/s and peak height 10 mV (top); cyclic voltammogram at scan rate of 200 mV/s (bottom).

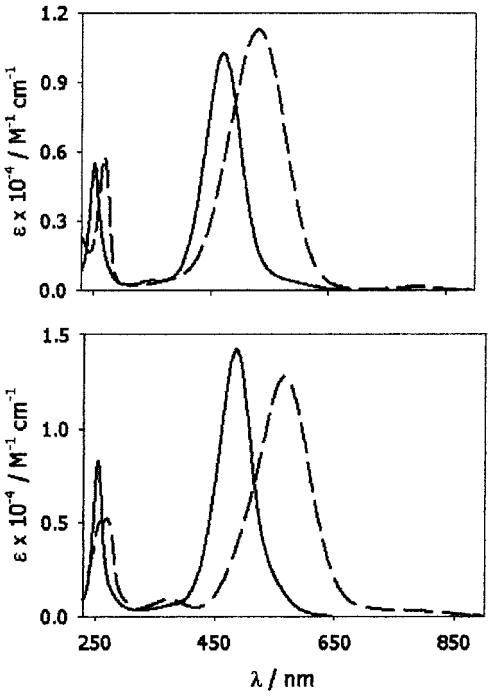

Figure 2. Absorption spectra of free (solid line) and protonated (dashed line) forms of $[Ru(NH_3)_5(pyz)]^{2+}$ (top) and of *trans*-$[Ru(NH_3)_4(pyz)_2]^{2+}$ (bottom) complexes in aqueous solution.

The IR spectra are in agreement with those already observed[35,38] for similar compounds, and the assignment[39] of some bands is also supported by the spectra of perdeuterated species recovered from NMR samples. In fact, absorption maxima in the range 3300−3100 (ν_{NH}), 1630−1620, and around 1300 cm^{-1} (ν_{NH}) move down to 2440−2300, 1200, and 1000 cm^{-1}, respectively.

Oxidation of Ru_3^{6+} with 2 equiv of Ce(IV) in 1.0 M H_2SO_4 yields a microcrystalline solid that was identified as Ru_3^{8+} by IR and UV−vis spectroscopy and elemental analysis. The most intense band in the visible spectrum of the complex is superimposable, at the same concentration, with the one obtained after the addition of 2 Ce(IV) equiv to Ru_3^{6+} in the spectrometric cell (see later). Unfortunately, NMR analysis was prevented for solubility reasons, and attempts to isolate Ru_3^{8+} as a nitrate salt, to increase the solubility, failed: by treating Ru_3^{6+} with $Ce(NH_4)_2(NO_3)_6$ in 1 M HNO_3, the microcrystalline violet solid that immediately formed decomposed after a few minutes, giving a yellow solution. Most likely, the nitrate ion acts as an oxidant itself[32] giving rise to byproducts.

Electrochemistry. Cyclic voltammetry and differential pulse voltammetry of Ru_3^{6+}−P in 1.0 M H_2SO_4 (i.e., in conditions identical to those in which chemical oxidation has been carried out) are reported in Figure 1. Three monoelectronic, fully reversible, oxidation processes are observed at the following estimated potentials (mV, vs SCE): $E_{1/2}$ ($6^+/7^+$) = +(171 ± 3); $E_{1/2}$ ($7^+/8^+$) = +(285 ± 3); $E_{1/2}$ ($8^+/9^+$) = +(715 ± 3).

These values are in agreement with the results already obtained by von Kameke, Tom, and Taube[32] and are supported by the potential values obtained for the oxidation of $[Ru(NH_3)_5(pyz)]^{2+}$ and *trans*-$[Ru(NH_3)_4(pyz)_2]^{2+}$. Both complexes can give rise to a protonation equilibrium. The UV−vis spectra of the protonated and unprotonated species are reported in Figure 2; the pK_a values obtained by spectrophotometric titrations are 2.4 and 1.0, respectively. Furthermore, the oxidation products can be, in principle, either protonated or not.

For $[Ru(NH_3)_5(pyz)]^{2+}$, the observed (CV and DPV) value of $E_{1/2}$ = +(284 ± 2) mV vs SCE at natural pH should correspond to a process involving unprotonated species. In 1.0 M H_2SO_4, the oxidation process takes place, as expected, at higher potential values, and repeated CV experiments carried out at different scan rates (up to 5 V/s) showed that the process is affected by some chemical irreversibility, probably due to the slow deprotonation of the oxidized species. Considering only the highest scan rates, a value of $E_{1/2}$ = +(430 ± 10) mV vs SCE is obtained which can thus be attributed to the protonated/unprotonated couple. For comparison purposes, a value of $E_{1/2}$ = +479 mV for the protonated/protonated couple can be calculated[40] from the $E_{1/2}$ value obtained at natural pH and the pK_a values of the species (for the oxidized one, the literature[41] value of −0.8 has been used).

For *trans*-$[Ru(NH_3)_4(pyz)_2]^{2+}$, a value (CV and DPV) of $E_{1/2}$ = +(592 ± 2) mV vs SCE is obtained; it is worthy to note the observation that this value is unaffected by pH. Considering that the oxidized complex is unstable as a protonated species, this result might be interpreted by

(38) Seddon, E. A.; Seddon, K. R. *The Chemistry of Ruthenium*; Elsevier: Amsterdam, 1984.
(39) Nakanishi, K.; Solomon, P. H. *Infrared Absorption Spectroscopy*; Holden-Day, Inc.: San Francisco, CA, 1977.
(40) Lim, H. S.; Barclay, D. J.; Anson, F. C. *Inorg. Chem.* **1972**, *11*, 1460.
(41) Ford, P.; Rudd, De F. P.; Gaunder, R.; Taube, H. *J. Am. Chem. Soc.* **1968**, *90*, 1187.

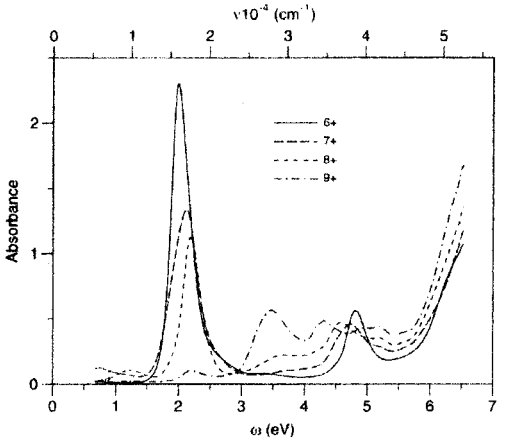

Figure 3. Measured spectra of 5×10^{-5} M Ru_3^{6+} in D_2O solution (1.0 M H_2SO_4) after successive stoichiometric additions of 0.1 M Ce(IV).

Table 1. NIR−Vis Spectral Data for the Trimetallic Species of Different Total Charges

species	ω_{max} (eV)	$\epsilon \times 10^{-3}$ (cm^2 mol^{-1})	fwhm (eV)
6+	1.99	46.0	0.35
7+	0.75	2.5	*a*
	2.12	26.7	0.55
8+	1.22	2.1	0.58
	2.18	22.5	0.33

[a] Only a little more than half of the band can be seen in the spectral window.

supposing that the reduced complex (monoprotonated or unprotonated) always approaches the electrode with its unprotonated pyrazine side. The obtained value is roughly in the middle between those reported by von Kameke, Tom, and Taube[32] (1.0 M H_2SO_4, $E_{1/2} = +0.85$ V vs NHE) and by Lim, Barclay, and Anson[40] (natural pH, $E_{1/2} = +0.78$ V vs NHE).

NIR−Vis Absorption Spectra of [*trans*-{$Ru(NH_3)_5pyz$}$_2$-$Ru(NH_3)_4$]$^{m+}$ ($m = 6-9$). NIR−vis spectra upon successive stoichiometric additions of Ce(IV) are reported in Figure 3. Measurements were made after each addition of 0.5 equiv, but for clarity, only the spectra corresponding to additions of full equivalents are reported. Absorption maxima, molar absorptivities, and bandwidths are summarized in Table 1.

In consequence of oxidation, the strong visible band moves to a shorter wavelength while its intensity decreases, as already observed.[32] The band is totally absent in the fully oxidized species.

In the NIR, after the addition of the first equivalent of oxidant ($Ru_3^{6+} \rightarrow Ru_3^{7+}$), a band appears at 0.7 eV, which disappears after the second equivalent is added ($Ru_3^{7+} \rightarrow Ru_3^{8+}$), while a band at 1.2 eV rises.

The addition of a third equivalent of the oxidant does not produce a complete conversion of Ru_3^{8+} ion, and an excess of at least 2 equiv of Ce(IV) is required to achieve a nearly complete oxidation to the Ru_3^{9+} ion. The band of Ru_3^{8+} at ~570 nm simply decreases in intensity, maintaining its shape, and no other band at a shorter wavelength is observed. After 2 days in the dark, Ru_3^{8+} ion is regenerated; further reduction with Zn amalgam gives quantitatively the Ru_3^{6+} ion.

The spontaneous reduction of the 9+ species is confirmed by comparing its spectrum with that of a sample of the 8+ species prepared as discussed in the previous section. The same experiment, performed in neutral solution, does not provide substantially different absorption patterns. This indicates that the $Ru_3^{8+} \rightarrow Ru_3^{9+}$ step does not cause any degradation of the trimetallic species, unlike Taube's hypothesis.[32] In fact, if degradation occurred, the resulting fragments having a terminal pyrazine should show well displaced visible bands in acidic or neutral solution.

Further assays have been made to give a better explanation of such behavior. First, it has been proven that there is not an equilibrium between the couples Ru_3^{8+}/Ru_3^{9+} and Ce^{4+}/Ce^{3+}, because the formation rate of Ru_3^{8+} is not affected by addition of large quantities of Ce(III) to the solution. Then, the possibility that the water solvent was directly involved in the redox system was explored. Indeed, when Ru_3^{6+} was treated under argon pressure with a large excess of Ce(IV), a large evolution of dioxygen was detected, and Ru_3^{8+} was recovered. Therefore, it is clear that the oxidation of Ru_3^{8+} by Ce(IV) competes with the reduction reaction of Ru_3^{9+} by water. Indeed, some other cases of catalytic oxidation of water mediated by Ru(III) complexes are known,[42] and mechanisms involving the coordination of water to the metallic center[42] or its association with a coordinated ligand[43] have been proposed.

Model. The observed NIR−vis spectra of the trinuclear pyrazine bridged Ru complex of various total charge can be investigated theoretically by a suitable electronic model Hamiltonian.[33] The effects of the coupling with nuclear degrees of freedom,[18−25] of relevance in determining the line shape profile, have not been considered for the purpose of the present work.

The model is very simple and takes into account only one orbital per site (site is defined as $Ru(NH_3)_5$ and pyz moieties), that is, the Ru d_{xz} orbital (with pyz in the plane *yz*, *z* being the Ru−pyz−Ru axis) for each Ru and the pyz π^* orbital for each pyz bridge, as shown.

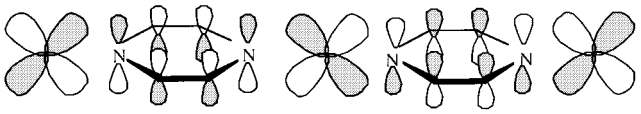

In fact, Ru(II) and Ru(III) have, respectively, $4d^6$ and $4d^5$ configurations, and it is well-known[23a,27] that the bridging ligand breaks the degeneracy of the t_{2g} orbitals, so that d_{xz} is the highest in energy: at zero order, the d_{xz} is occupied by two electrons for Ru(II) and one for Ru(III), while the pyz π^* is empty.

Within this scheme of few selected orbitals, one must take into account that pyz π^* and Ru d_{xz} are separate in energy and that electrons may hop between the two orbitals owing to the back-bonding interaction, which is the source of the electron delocalization. Finally, the effect of electron−

(42) (a) Ruttinger, W.; Dismukes, G. C. *Chem Rev*. **1997**, *97*, 1 and references therein. (b) Kinoshita, K.; Yagi, M.; Kaneko, M. *J. Mol. Catal. A: Chem*. **1999**, *142*, 1.
(43) Ledney, M.; Dutta, P. K. *J. Am. Chem. Soc*. **1995**, *117*, 7687.

electron Coulomb repulsion must be considered, at least when two electrons are in the same orbital. These ingredients can be incorporated in a two-band Hubbard Hamiltonian:[44]

$$H = \sum_{j,\sigma}^{N_{site}} \epsilon_j n_{j,\sigma} + t \sum_{j,\sigma}^{N_{site}-1} (a_{j,\sigma}^{+} a_{j+1,\sigma} + h.c.) + U_{Ru} \sum_{j}^{Ru_{site}} n_{j,\uparrow} n_{j,\downarrow} + U_{pyz} \sum_{j}^{pyz_{site}} n_{j,\uparrow} n_{j,\downarrow} \quad (1)$$

where $a_{j,\sigma}^{+}$ ($a_{j,\sigma}$) is the creation (annihilation) operator for one electron in the orbital of site j with spin σ, $n_{j,\sigma} = a_{j,\sigma}^{+} a_{j,\sigma}$ is the number operator for the spin orbital $j\sigma$, t is the $d_{xz}-\pi^*$ resonance integral (or hopping), $\epsilon_j = \epsilon_{pyz}$, ϵ_{Ru} ($\Delta = \epsilon_{pyz} - \epsilon_{Ru}$) is the site energy, U_j (j = Ru, pyz) is the on-site repulsion term, $N_{site} = N_{Ru} + N_{pyz}$ is the total number of sites and also the number of orbitals (five in the present case).

The model Hamiltonian of eq 1 is diagonalized on the full reduced configurational space made by

$$N = \binom{N_{site}}{N_{el\uparrow}} \binom{N_{site}}{N_{el\downarrow}}$$

basis states ($N_{el\uparrow}/N_{el\downarrow}$ = total number of electron with spin up/down; $N_T = N_{el\uparrow} + N_{el\downarrow} = N_{Ru(III)} + 2N_{Ru(II)}$). For each ion, the combination of up and down spins that gives the minimal value of S_z is considered, and the configurations corresponding to the highest value of S^2 are not eliminated: for the trimetallic species of the present work, there are 100 basis states for $Ru_3^{6+}-Ru_3^{8+}$ and 50 for Ru_3^{9+}, respectively.

The dipole operator, in second quantization form, can be derived for the sites at fixed distance (in units of the Ru−pyz distance) as

$$\mu = \sum_{j,\sigma}^{N_{site}} n_{j,\sigma} \left(j - \frac{N_{site} + 1}{2} \right) \quad (2)$$

From eqs 1 and 2, once the values of the four parameters in eq 1 are given, energies, eigenfunctions, and spectra of the different ions can be obtained. Notice that it is important that these values be the same for all ions, to be sure that the model indeed catches the essential physics of the systems and does not represent just a simulation.

Results of Computations. For the computation of the NIR−vis absorption spectra of the Ru_3^{m+} (m = 6−9) complexes according to eqs 1 and 2, two different sets of parameters (in eV) have been utilized:

(a) $t = -0.73$ $U_{Ru} = 4.62$ $U_{pyz} = 2.5$ $\Delta = 5.06$

(b) $t = -1.03$ $U_{Ru} = 5.02$ $U_{pyz} = 2.5$ $\Delta = 5.46$

Set a, optimized for the bimetallic pyrazine-bridged systems (the Creutz−Taube ion and its homovalent counterparts),[28c,29,33c] is also used for the study of 4,4′-bipyridine-bridged Ru dinuclear complexes,[29,33c] as well as in the study of third harmonic generation in polymetallic systems.[3a] Set b derives from set a, but the resonance term, in absolute value, has been increased by 0.3 eV, and both the Coulomb term and the band gap have also been increased by 0.4 eV.

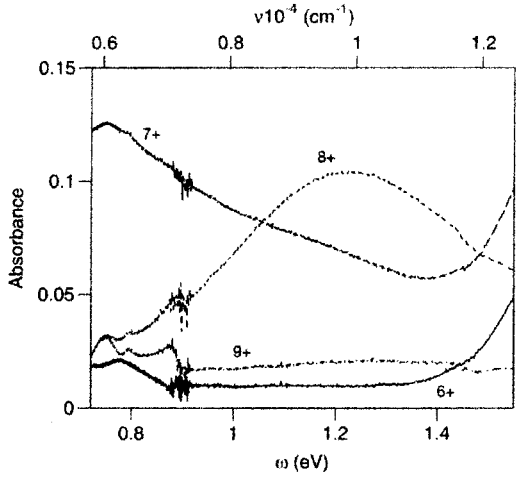

Figure 4. Enlargement of the NIR portion of the spectra reported in Figure 3.

It can be seen that the essential features experimentally observed, such as the behavior in the NIR and in the vis regions, as well as the nature of the eigenstates involved in the transitions, do not strongly depend on the choice between sets a and b. Although this stability with respect to the value of the parameters is a reason for confidence in a wide applicability of the model, it cannot be forgotten that in real experiments solute−solvent interactions play a significant role for these systems.[30c,30e,45,46] In the framework of the model, which focuses on the solute molecule alone, these effects can be taken into account only by varying the value of the parameters. As discussed below, the parameters of set b fit the positions of the observed bands better than those of set a.

In Figure 5, the NIR−vis spectra computed with the two sets of parameters are reported. They should be compared with the experimental results of Figures 3 and 4. Although the relative intensities of the NIR versus vis bands are too high in the computations with respect to the experiments, the spectral changes upon oxidation are very well reproduced. Indeed, the 6+ species only shows absorption in the vis region, while oxidation to 7+ brings the appearance of a NIR band, which is blue-shifted by further oxidation to 8+; the 9+ species does not show any absorption below 3 eV.

The vis absorption has a double component for the 6+ and 7+ ions (the two computed lines should merge into a single wide band if nuclear degrees of freedom were also considered), which explains the observed difference in the line shape profile of the 6+ and 7+ species as compared to that of the 8+ species, which is narrower in the experiment

(44) Hubbard, J. *Proc. R. Soc. London* **1964**, *285*, 542.

(45) Chen, P.; Meyer, T. J. *Chem. Rev.* **1998**, *98*, 1439.

(46) (a) Stavrev, K. K.; Zerner, M.; Meyer, T. J. *J. Am. Chem. Soc.* **1995**, *117*, 8684. (b) Pearl, G. M.; Zerner, M. *J. Am. Chem. Soc.* **1996**, *118*, 2059. (c) Shin, Y. K.; Brunschwig, B. S.; Creutz, C.; Newton, M. D.; Sutin, N. *J. Phys. Chem.* **1996**, *100*, 1104. (d) Zeng, J.; Hush, N. S.; Reimers, J. R. *J. Am. Chem. Soc.* **1996**, *118*, 2059. (e) Zeng, J.; Hush, N. S.; Reimers, J. R. *J. Phys. Chem.* **1996**, *100*, 19292. (f) Cacelli, I.; Ferretti, A. *J. Chem. Phys.* **1998**, *109*, 8583. (g) Cacelli, I.; Ferretti, A. *J. Phys. Chem.* **1999**, *103*, 4438.

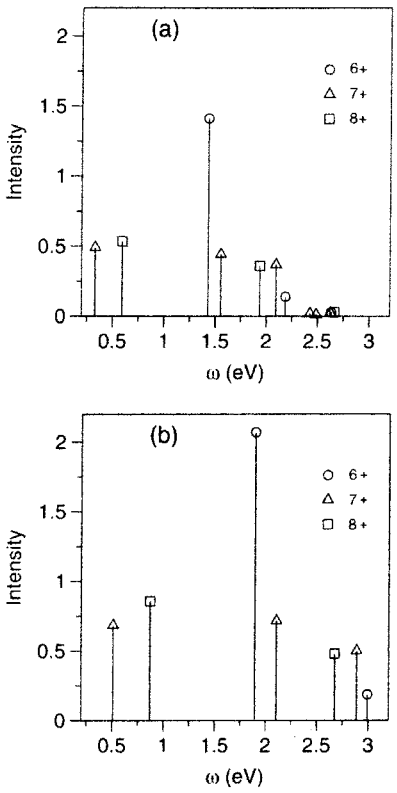

Figure 5. Computed spectra of Ru_3^{m+} at various total charge *m*, as obtained by the two-band Hubbard model with the two sets of parameters a and b (see text and Table 2).

(Figure 3). The vis band is blue-shifted upon oxidation as in the experiments; this effect has been observed also in cyanide-bridged trimetallic species.[17]

In Table 2, the analyses of the ground and excited states involved in the observed spectra are reported. From the comparison of parts a and b of the table, it is very evident that the two sets of parameters do not provide substantially different results as far as the nature of the transitions is concerned.

In the ground state, all the 6−8+ species essentially have the same charge distribution on the three metal centers. Only the 8+ ion seems to show a weak effect due to the different chemical environment of the central ruthenium in comparison with the two external ones, with a slight stabilization of the (3,2,3) configuration with respect to the (2,3,3) and (3,3,2) configurations: this results in a ground state in which the terminal ruthenium atoms are more positively charged than the central one (see columns 6 and 8 in Table 2 for the 8+ species). Furthermore, although the ground state has essentially a metallic character, it is evident that a Ru−pyz d−π* back-bonding interaction occurs, because the pyz rings become negatively charged.

As expected, all the bands exhibited by the different species in the vis region above 1.5 eV are metal-to-ligand charge transfer (MLCT) bands where a fraction of electronic charge (and not a whole electron) is transferred from the metal to the ligand. The two components of these bands observed for the 6+ and 7+ ions do not substantially differ in the amount of electronic charge transferred but in the charge distribution on the three metals (Table 2). For the

Table 2. Analysis of the Ground and Excited States Which Contribute to the NIR−Vis Spectrum As Obtained by the Model Hamiltonian of Equation 1 with the Two Sets of Parameters a and b (See Text)

ion	state	type	ΔE (eV)	ΔE (eV) exptl	$Ru_1 = Ru_3$ charge	$pyz_1 = pyz_2$ charge	Ru_2 charge
a. $t = -0.73$, $U_{Ru} = 4.62$, $U_{pyz} = 2.50$, $\Delta = 5.06$ (all in eV)							
	g				2.31	−0.49	2.35
6+	e_1	MLCT	1.429	2.0	2.42	−0.76	2.67
	e_2	MLCT	2.186		2.48	−0.70	2.46
	g				2.62	−0.43	2.64
	e_1	IT	0.332	0.7	2.67	−0.37	2.42
7+	e_2	MLCT	1.554	2.1	2.90	−0.66	2.54
	e_3	MLCT	2.094		2.78	−0.65	2.75
	g				2.94	−0.26	2.64
8+	e_1	IT	0.593	1.2	2.71	−0.22	3.02
	e_2	MLCT	1.936	2.2	3.01	−0.52	3.01
b. $t = -1.03$, $U_{Ru} = 5.02$, $U_{pyz} = 2.50$, $\Delta = 5.46$ (all in eV)							
	g				2.35	−0.54	2.39
6+	e_1	MLCT	1.895	2.0	2.44	−0.79	2.70
	e_2	MLCT	2.993		2.49	−0.74	2.50
	g				2.65	−0.48	2.67
	e_1	IT	0.509	0.7	2.69	−0.42	2.46
7+	e_2	MLCT	2.105	2.1	2.89	−0.68	2.58
	e_3	MLCT	2.889		2.79	−0.68	2.78
	g				2.95	−0.30	2.70
8+	e_1	IT	0.868	1.2	2.73	−0.25	3.03
	e_2	MLCT	2.674	2.2	3.02	−0.53	3.02

8+ ion, the charge transfer essentially appears to occur from the central Ru to the two nearest pyz moieties.

Intervalence (IT) or metal-to-metal charge transfer (MMCT) transitions are found in the low energy part of the spectra of the mixed-valence species. For the 7+ ion, the transition is very similar to that observed in the Creutz−Taube ion: the involved excited state has about the same charge distribution on the metals as in the ground state, with the exception of a very small ligand-to-metal charge transfer (LMCT) (the central metal seems to be the most involved); the excited state can be mainly seen as the antisymmetric combination of (2,2,3) and (3,2,2) configurations, while the ground state can be seen as the symmetric one. The situation is different for the 8+ ion, because the dominant configurations, in which the metallic character prevails, respectively, are the (3,2,3) one, in the ground state, and the antisymmetric combination of (3,3,2) and (2,3,3), in the excited state. The MMCT is, therefore, essentially an electronic charge transfer from the central to the terminal Ru atoms, again with a slight LMCT component (Table 2) as for the 7+.

Two different MMCTs are also reported by Endicott and co-workers for CN-bridged trinuclear compounds.[17] However, while their system formally containing two Ru(III) and one Ru(II) centers indeed shows only the central-to-terminal charge transfer, as in the Ru_3^{8+} analogue presented here, the one that contains one Ru(III) and two Ru(II) centers does exhibit not only the same band observed for the Ru_3^{7+} ion but also a band which can be associated with the central-to-terminal charge transfer.

Conclusions

In the present article, a theoretical and experimental study is reported concerning the NIR−vis optical properties of a

trinuclear pyrazine-bridged Ru complex as a function of the oxidation state of the metals. This study is motivated by the need for investigating and understanding the optical properties of metal−ligand complexes as the nuclearity increases, and in this perspective, it may contribute to the knowledge of mixed-valence compounds.

The complex has been synthesized and isolated as a 6+ ion [all Ru(II)] in good yield and fully characterized by spectroscopic, electrochemical, and elemental analysis. The 8+ species has also been isolated to confirm the assignment of the NIR−vis bands to the penultimate oxidation state of the trimetallic complex.

Upon oxidation by Ce(IV), the spectra show the typical transfer of spectral weight from the MLCT band to NIR bands. Two distinct bands having mainly metallic character are observed for the two mixed-valence 7+ and 8+ species. This behavior differs from that observed in cyanide-bridged complexes[17] where both bands are observed for the 7+ system.

In the last oxidation step ($Ru_3^{8+} \rightarrow Ru_3^{9+}$), Ce(IV) is consumed in a large excess. It has been demonstrated that this does not occur as a consequence of decomposition or side reactions but because of the reduction of the 9+ species by water.

The experimental results have been interpreted in terms of a simple two-band Hubbard model which is shown to account, with the same set of parameters, for the whole set of measurements.

As far as theoretical and experimental results are concerned, the trinuclear system shows strong charge delocalization, like the more studied Creutz−Taube dinuclear one. Indeed, the ground state for the different ions, as investigated according to the Hubbard model Hamiltonian, has the electronic charge distributed on the three metals: only the 8+ species shows that the (3,2,3) configuration is a little more favored. Furthermore, the pyrazine bridges contribute to the ground state with their π^* orbitals: the negative charge present on them indicates a strong back-bonding interaction.

The NIR band for the 7+ species has the same nature as that observed in the 5+ dinuclear compound, but the increased nuclearity causes a slight red-shift of the band and a sensible decrease of its intensity. For the 8+ species, a different band with metallic character is observed, as a consequence of the different charge distribution. In the visible, the MLCT band, which is blue-shifted and decreased in intensity with respect to the 6+ species, can be associated with the transfer of less than half an electron.

Note. In the opinion of one of the anonymous reviewers, the experimental spectroscopic and electrochemical data might be accounted for using a weakly coupled valence-trapped model, rather than the one presented here.

Acknowledgment. We wish to express our gratitude to Dr. Francesco Barigelletti (FRAE-CNR, Bologna) for the help in the NIR-vis measurements, as well as for his kind and wise suggestions. The help of Dr. Felicia D'Andrea (Dipartimento di Chimica Bioorganica e Biofarmacia, University of Pisa) in running NMR spectra is also acknowledged. We wish also to thank Prof. John F. Endicott (Wayne State University) for stimulating discussions on his cyanide-bridged compounds. Financial support from Italian CNR and Italian Ministry for University and Scientific and Technological Research (Cofin'99 project) is gratefully acknowledged.

IC010869Y